

Ab initio calculations of p -shell nuclei up to N^2 LO in chiral Effective Field Theory

Pieter Maris

Dept. of Physics and Astronomy, Iowa State University, Ames, IA 50011, USA

E-mail: pmaris@iastate.edu

Abstract. Nuclear structure and reaction theory are undergoing a major renaissance with advances in many-body methods, realistic interactions with greatly improved links to Quantum Chromodynamics, the advent of high performance computing, and improved computational algorithms. State-of-the-art two- and three-nucleon interactions obtained from chiral Effective Field Theory provide a theoretical foundation for nuclear theory with controlled approximations. With highly efficient numerical codes, tuned to the current generation of supercomputers, we can perform ab-initio nuclear structure calculations for a range of nuclei to a remarkable level of numerical accuracy, with quantifiable numerical uncertainties. Here we present an overview of recent results for No-Core Configuration Interaction calculations of p -shell nuclei using these chiral interactions up to next-to-next-to-leading order, including three-body forces. We show the dependence of the ground state energies on the chiral order; we also present excitation spectra for selected nuclei and compare the results with experimental data.

1. Ab Initio Nuclear Structure and High Performance Computing

A microscopic theory for the structure and reactions of atomic nuclei poses formidable challenges for high-performance computing. A nucleus with Z protons and N neutrons is a self-bound quantum many-body system with $A = N + Z$ strongly interacting nucleons. The interactions feature both attractive and repulsive contributions along with significant spin and angular momentum dependence. Furthermore there are both short-range and long-range terms in the interaction, and in addition to nucleon-nucleon (NN) interactions, one also needs suitable three-nucleon forces (3NFs), and possibly even higher many-body interactions. The corresponding Hamiltonian can be written as

$$\hat{\mathbf{H}} = \sum_{i < j} \frac{(\vec{p}_i - \vec{p}_j)^2}{2m A} + \sum_{i < j} V_{ij} + \sum_{i < j < k} V_{ijk} + \dots \quad (1)$$

where m is the nucleon mass, which we take to be equal for protons and neutrons. The nuclear wave functions are the solutions of the many-body Schrödinger equation

$$\hat{\mathbf{H}} \Psi(\vec{r}_1, \dots, \vec{r}_A) = E \Psi(\vec{r}_1, \dots, \vec{r}_A) \quad (2)$$

at discrete energy levels E .

In No-Core Configuration Interaction (NCCI) nuclear structure calculations [1] the wave function Ψ of a nucleus consisting of A nucleons is expanded in an A -body basis of Slater

determinants Φ_k of single-particle wave functions $\phi_{nljm}(\vec{r})$. Here, n is the radial quantum number, l the orbital motion, j the total spin from orbital motion coupled to the intrinsic nucleon spin, and m the spin-projection. The Hamiltonian \hat{H} is also expressed in this basis and thus the many-body Schrödinger equation becomes a matrix eigenvalue problem; for $A > 4$ and NN plus 3N interactions, this matrix is sparse. The eigenvalues of this matrix are approximations to the energy levels, to be compared to the experimental binding energies and spectra, and the corresponding eigenvectors to the nuclear wave functions. Although the wave functions themselves are not observable, they can be employed to evaluate additional physical observables.

Conventionally, one uses a harmonic oscillator (HO) basis with energy parameter $\hbar\omega$ for the single-particle wave functions. A convenient and efficient truncation of the complete (infinite-dimensional) basis is a truncation on the total number of HO quanta: the basis is limited to many-body basis states with $\sum_A N_i \leq N_0 + N_{\max}$, with N_0 the minimal number of quanta for that nucleus and N_{\max} the truncation parameter. (Even (odd) values of N_{\max} provide results for natural (unnatural) parity.) Numerical convergence toward the exact results for a given Hamiltonian is obtained with increasing N_{\max} , and is marked by approximate N_{\max} and $\hbar\omega$ independence. In practice we use extrapolations to estimate the binding energy in the complete (but infinite-dimensional) space [2, 3, 4, 5, 6], based on a series of calculations in finite bases.

The rate of convergence depends both on the nucleus and on the interaction. For realistic interactions, the dimension of the matrix needed to reach a sufficient level of convergence is in the billions, and the number of nonzero matrix elements is in the tens of trillions, which saturates available storage on current computing facilities. All NCCI calculations presented here were performed on the Cray XC30 Edison and Cray XC40 Cori at NERSC and the IBM BG/Q Mira at Argonne National Laboratory, using the code MFDn [7, 8].

2. Nuclear Interactions from Chiral Effective Field Theory

Chiral Effective Field Theory (χ EFT) allows us to derive nuclear interactions (and the corresponding electroweak current operators) in a systematic way [9, 10, 11]. The chiral expansion is by no means unique: e.g. different choices for the functional form of the regulator and/or different choices for the degrees of freedom lead to different χ EFT interactions. With the LENPIC collaboration [12, 13, 14] we use the same χ EFT interactions for ab initio calculations ranging from nucleon-nucleon and nucleon-deuteron scattering to the structure of medium-mass nuclei. Specifically, here we use the semilocal coordinate-space regularized chiral potentials of Refs. [15, 16] to calculate the binding energies and spectra of p -shell nuclei. The leading order (LO) and next-to-leading order (NLO) contributions are given by NN-only potentials while 3NFs appear first at next-to-next-to-leading order (N^2 LO) in the chiral expansion [10, 11]. Four-nucleon forces are even more suppressed and start contributing at N^3 LO. The chiral power counting thus provides a natural explanation of the observed hierarchy of nuclear forces.

The Low-Energy Constants (LECs) in the NN-only potentials of Refs. [15, 16] have been fitted to nucleon-nucleon scattering, without any input from nuclei with $A > 2$. The 3NFs at N^2 LO involve two LECs which govern the strength of the one-pion-exchange-contact term and purely contact 3NF contributions. Conventionally, these LECs are expressed in terms of two dimensionless parameters c_D and c_E . Obviously, these LECs cannot be fixed from nucleon-nucleon scattering; they have to be fitted to select 3-body (or higher A -body) observables. We follow the commonly adopted practice [17, 18, 19, 20] and use the ^3H binding energy as one of the observables; this gives us a correlation between c_D and c_E .

A wide range of observables has been considered in the literature to constrain the remaining LEC. In Ref. [14] different ways to fix this LEC in the 3-nucleon sector were explored, and it was shown that it can be reliably determined from the minimum in the differential cross section in elastic nucleon-deuteron scattering at intermediate energies. This allows us to make parameter-free calculations for $A \geq 4$ nuclei. In these proceedings we present an overview of the ground

state energies for all stable p -shell nuclei (excluding mirror nuclei), as well as excitation spectra for selected nuclei up to $A = 12$, all obtained with the same semilocal regulator $R = 1.0$ fm and the same LECs. Specifically, the LECs values for the 3NFs at N²LO are $c_D = 7.2$ and $c_E = -0.671$, as determined in Ref. [14]. Application of these interactions to nucleon-deuteron scattering can be found in Refs. [12, 13] for NN-only potentials, along with selected properties of light- and medium-mass nuclei, and in Ref. [14] including the 3NFs at N²LO.

3. Ground State Energies for p -shell Nuclei

Here we present our results for the ground state energies of the stable p -shell nuclei, excluding mirror nuclei, all obtained with the same semilocal chiral interactions up to N²LO. In Fig. 1 we show the ground state ($J^P = 1^+$) energy of ${}^6\text{Li}$ as function of the HO basis parameter $\hbar\omega$ for a range of N_{max} values. With NN-only potentials, we can perform calculations up to $N_{\text{max}} = 18$ for $A = 6$ nuclei. This is sufficient to achieve a reasonable level of convergence, as can be seen from the left three panels of Fig. 1. With 3NFs however, we are limited to significantly smaller bases, and in order to improve the numerical convergence with basis size we therefore first perform a Similarity Renormalization Group (SRG) transformation [21, 22, 23] on the Hamiltonian. The right-most panel of Fig. 1 shows results for the ground state energy of ${}^6\text{Li}$ at N²LO including 3NFs at a very modest SRG flow parameter $\alpha = 0.02$ fm⁴ (note that $\alpha = 0$ correspond to the original Hamiltonian, without SRG), for calculations up to $N_{\text{max}} = 12$. Indeed, the convergence with increasing N_{max} is significantly improved with this SRG-evolved interaction compared to the bare NN-only interactions at NLO and N²LO. At $N_{\text{max}} = 12$ the level of convergence is already comparable to that of the bare NLO and N²LO potentials at $N_{\text{max}} = 16$. Also note that the variational minimum in $\hbar\omega$ shifts to lower values due to the SRG evolution.

In Fig. 2 we show the ground state energies of ${}^7\text{Li}$ (left, $J^P = \frac{3}{2}^-$) and ${}^{10}\text{B}$ (right, $J^P = 3^+$) as function of N_{max} at fixed $\hbar\omega$ values close to the variational minimum with the N²LO interaction with and without explicit 3NFs. Based on these results in finite bases, we can use extrapolations to the complete (infinite-dimensional) basis. Here we use a three parameter fit at fixed $\hbar\omega$ at or just above the variational minimum

$$E(N_{\text{max}}) \approx E_{\infty} + a \exp(-bN_{\text{max}}), \quad (3)$$

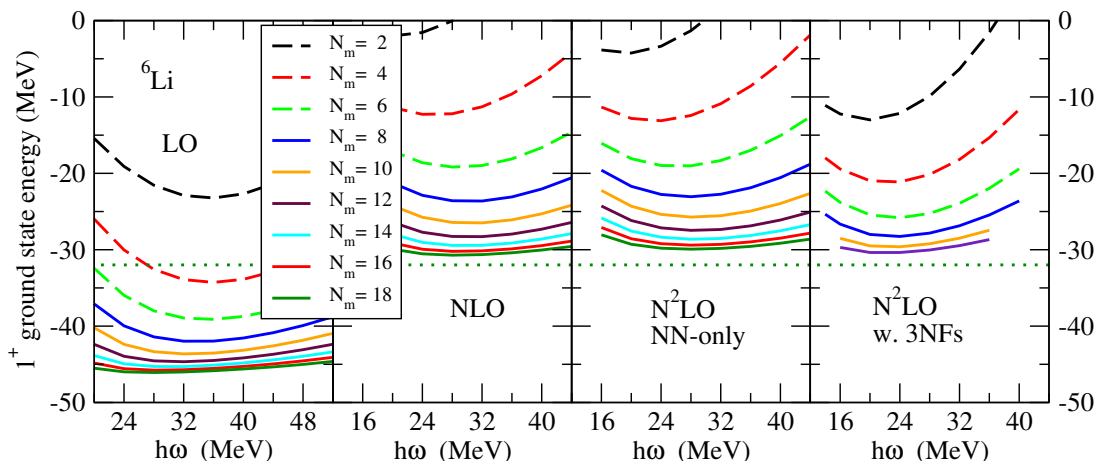


Figure 1. (Color online) Calculated ground state energy of ${}^6\text{Li}$ using chiral LO, NLO, and N²LO interactions at $R = 1.0$ fm as function of the basis HO parameter $\hbar\omega$ for $N_{\text{max}} = 2$ to 18 for NN-only potentials (left 3 panels) and at N²LO w. 3NFs, SRG-evolved to $\alpha = 0.02$ fm⁴ for $N_{\text{max}} = 2$ to 12 (right-most panel). The dotted horizontal line is the experimental value.

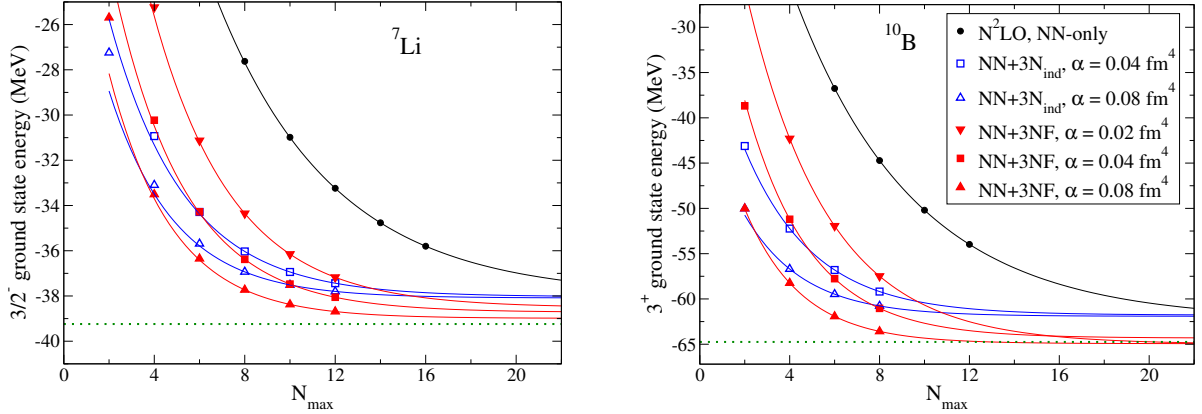


Figure 2. (Color online) Calculated ground state energies using chiral N²LO interactions at $R = 1.0$ fm as function of N_{max} at the variational minimum in $\hbar\omega$ for ${}^7\text{Li}$ (left) and ${}^{10}\text{B}$ (right). The dotted horizontal line is the experimental value.

which seems to work well for a range of interactions and nuclei [2, 24, 25]. The lines in Fig. 2 correspond to the extrapolating function fitted to the three highest available N_{max} values.

Again, with the SRG-evolved interactions the ground state energies converge more rapidly with N_{max} than with the bare (black dots and curves) NN-only N²LO interaction. However, as a consequence of the SRG transformation, our results do depend on the SRG flow parameter α , because we do not incorporate any induced interactions beyond 3NFs. Without explicit 3NFs, this dependence seems to be negligible, and typically less than the extrapolation uncertainty – the bare NN-only N²LO interaction and the two SRG-evolved interaction with induced 3NFs extrapolate to approximately the same value. On the other hand, with explicit 3NFs there is a weak but noticeable dependence on the SRG parameter α , as can be seen by the spread of the red extrapolation curves in Fig. 2. This α dependence is due to induced 4-body (and higher-body) interactions which we have neglected.

In Table 1 we summarize our results up to N²LO for the ground state energies of stable p -shell nuclei, excluding mirror nuclei, extrapolated to the complete basis. Our estimate of the extrapolation uncertainty is based on the difference with smaller N_{max} extrapolations, as well as the basis $\hbar\omega$ dependence over an 8 to 12 MeV span in $\hbar\omega$ values around the variational minimum, adjusted to be at least 20% of the difference with the variational minimum [13].

With NN-only potentials we use the bare interaction up to $A = 10$, for which we can perform calculation at $N_{\text{max}} = 12$ or higher. For select nuclei with $11 \leq A \leq 16$ we use the SRG-evolved interaction at $\alpha = 0.04$ fm⁴ with induced 3NFs for NN-only potentials up to $N_{\text{max}} = 8$. At N²LO with explicit 3NFs we present results with SRG-evolved interactions at both $\alpha = 0.04$ fm⁴ and $\alpha = 0.08$ fm⁴. As expected, the calculations at $\alpha = 0.08$ fm⁴ are better converged, and have therefore a smaller extrapolation uncertainty than those at $\alpha = 0.04$ fm⁴. The anticipated α dependence appears to be of the same order of magnitude as the extrapolation uncertainty.

Generally, the agreement with the experimental binding energies improves as one goes from LO to NLO to N²LO. At LO all p -shell nuclei are significantly overbound, but at N²LO the binding energies of nuclei up to $A = 12$ are within few percent of the experimental values. As A increases beyond $A = 12$, the nuclei become more and more overbound – ${}^{12}\text{C}$ is overbound by about 3% whereas ${}^{16}\text{O}$ is overbound by about 13%. The overbinding of ${}^{16}\text{O}$ is significantly larger than the estimated chiral truncation uncertainty [13], even with the inclusion of the explicit 3NFs [14], and it is as of yet unclear what the origin of this overbinding is.

At NLO and higher, we obtain the correct spin and parity for the ground states of most p -shell

Table 1. Ground state energies of stable $A = 4$ to 16 nuclei with χ EFT interactions up to N²LO using $R = 1.0$ fm [13, 14]. The uncertainty estimate is only the extrapolation uncertainty in the many-body calculation, and does not include the chiral truncation error, nor uncertainties in the LECs. Entries with an asterisk * indicate excited states for nuclei where the calculated and experimental ground states have different J^P . Experimental values are extracted from Ref. [26].

Nucleus	J^P	LO NN-only	NLO NN-only	N ² LO NN-only	N ² LO including 3NFs $\alpha = 0.04$ fm ⁴ $\alpha = 0.08$ fm ⁴		expt.
⁴ He	0 ⁺	−45.453(6)	−28.533(4)	−28.11(1)	−28.202(5)	−28.298(2)	−28.296
⁶ He	0 ⁺	−43.2(2)	−28.7(2)	−27.9(2)	−28.55(15)	−28.79(8)	−29.27
⁶ Li	1 ⁺	−46.7(1)	−31.6(2)	−31.0(2)	−31.49(16)	−31.72(6)	−31.99
⁷ Li	$\frac{3}{2}^-$	−57.1(2)*	−38.7(3)	−38.0(4)	−38.72(16)	−38.99(6)	−39.24
⁸ He	0 ⁺	−39.8(6)	−29.7(5)	−27.8(6)	−29.5(3)	−29.9(2)	−31.41
⁸ Li	2 ⁺	−55.7(5)	−40.3(7)	−39.0(8)	−40.4(4)	−40.7(2)	−41.28
⁸ Be	0 ⁺	−87.7(4)	−56.0(7)	−55.4(9)	−55.6(5)	−56.1(3)	−56.50
⁹ Li	$\frac{3}{2}^-$	−57.1(4)	−43.9(7)	−41.7(8)	−43.9(4)	−44.0(2)	−45.34
⁹ Be	$\frac{3}{2}^-$	−84.7(7)	−58.0(1.4)	−56.4(1.5)	−57.5(5)	−58.0(3)	−58.16
¹⁰ Be	0 ⁺	−92.2(8)	−65.2(1.5)	−62.8(1.7)	−64.1(9)	−64.9(5)	−64.98
¹⁰ B	3 ⁺	−88.1(1.2)*	−64.6(1.5)*	−62.3(1.7)*	−64.3(8)	−64.9(5)	−64.75
¹⁰ B	1 ⁺	−93.9(8)	−64.9(1.8)	−63.1(1.9)	−63.1(1.0)*	−64.1(8)*	−64.03*
		SRG evolved to $\alpha = 0.04$ fm ⁴			$\alpha = 0.04$ fm ⁴	$\alpha = 0.08$ fm ⁴	
¹¹ Be	$\frac{1}{2}^+$	—	—	—	−64.7(1.3)*	−65.4(8)*	−65.48
¹¹ Be	$\frac{1}{2}^-$	—	—	—	−65.8(1.2)	−65.7(8)	−65.16*
¹¹ B	$\frac{3}{2}^-$	−108.(1.)	−76.8(6)	−73.9(7)	−77.2(9)	−77.7(5)	−76.21
¹² Be	0 ⁺	—	—	—	−68.9(1.4)	−69.8(9)	−68.65
¹² B	1 ⁺	−111.(1.)*	−82.6(8)	−78.6(8)	−81.9(9)*	−82.5(5)*	−79.58
¹² B	2 ⁺	−111.(1.)*	−82.3(9)*	−77.8(7)*	−82.8(9)	−83.2(5)	−78.63*
¹² C	0 ⁺	−139.(1.)	−95.5(7)	−92.7(6)	−94.7(1.0)	−95.5(5)	−92.16
¹³ B	$\frac{3}{2}^-$	—	—	—	−89.5(1.0)	−90.3(7)	−84.45
¹³ C	$\frac{1}{2}^-$	—	—	—	−104.7(1.0)	−104.4(4)	−97.11
¹⁴ C	0 ⁺	—	—	—	−116.0(1.3)	−116.1(5)	−105.28
¹⁴ N	1 ⁺	—	—	—	−117.3(1.3)	−117.4(4)	−104.66
¹⁵ N	$\frac{1}{2}^-$	—	—	—	−130.4(1.6)	−131.0(6)	−115.49
¹⁶ O	0 ⁺	−223.2(4)	−152.(1.)	−146.(1.)	−144.(2.)	−145.2(8)	−127.62

nuclei – the exceptions are ¹⁰B, ¹¹Be, and ¹²B, for which we include both the experimental and the calculate ground states in Table 1. For ¹⁰B, the NN-only interactions produce a $J^P = 1^+$ ground state, whereas the experimental ground state has $J^P = 3^+$. With the consistent explicit 3NFs at N²LO we are able to reproduce the experimental ground state for ¹⁰B, in agreement with previous studies of ¹⁰B with χ EFT interactions [19, 25]. For ¹²B the situation is the opposite: at NLO and N²LO without the 3NFs we do find the correct ground state, $J^P = 1^+$, but adding the 3NFs to the N²LO NN potential leads to a ground state with $J^P = 2^+$, and the $J^P = 1^+$ state becomes the first excited state, with an excitation energy of about 1 MeV. It remains to

be seen whether or not this discrepancy gets resolved at higher order in the chiral expansion.

The situation in ^{11}Be is different: here we have a nucleus with *parity inversion*, that is, the ground state has the opposite parity of what one would expect based on the shell-model. In NCCI calculations the 'natural' and 'unnatural' parity states are expressed in bases with even or odd N_{max} values respectively. For ^{11}Be that means the negative parity states are calculated in bases with even N_{max} and the positive parity states in bases with odd N_{max} . We then perform an extrapolation to the complete basis for the lowest state with even N_{max} as well as for the lowest state with odd N_{max} . This leads to the energies listed in Table 1 for the $\frac{1}{2}^{+}$ state (the experimental ground state) and for the $\frac{1}{2}^{-}$ state (the lowest natural parity state). Although the latter has a lower energy in our calculations, the difference with that of the $\frac{1}{2}^{+}$ is less than the extrapolation uncertainty, and within their uncertainties, both energies agree with the experimental values. In order to reliably determine which of these two states is the ground state we should use more sophisticated calculational methods for this system and follow e.g. the approach discussed in Ref. [27] for ^{11}Be .

4. Excitation Spectra for p -shell Nuclei

In addition to the ground state energies, we also obtain the energy levels of excited states. The energy differences with the ground state generally converge significantly better than the actually binding energies of excited states, at least for states of the same parity. In Fig. 3 we show the low-lying spectra of ^6Li and ^7Li as function of the HO basis parameter $\hbar\omega$ for several of N_{max} values. Again, with NN-only potentials we achieve a reasonable level of convergence, in particular for narrow excited states like the 3^{+} state in ^6Li and the $\frac{1}{2}^{-}$ and $\frac{7}{2}^{-}$ states in ^7Li . The persistent increase of the excitation energies of with increasing $\hbar\omega$ for the higher excited states suggest that these are (significantly) broader, and therefore poorly converging in a HO basis. Indeed, the two 2^{+} states in ^6Li are broad; and although the 0^{+} in ^6Li (the analog state of ^6He) is narrow, in our calculations with NN-only interactions up to N^2LO , ^6He is not or barely bound, see Table 1; hence, with these interactions this state will be broad and poorly converging.

At LO the spectra do not agree with experiment – most excitation energies are too large, and often the order of the states is incorrect: e.g. in ^7Li the ground state, $\frac{3}{2}^{-}$, and the first excited state, $\frac{1}{2}^{-}$, are essentially degenerate. Indeed, the LO potential is not very realistic – not only is it significantly too attractive (it overbinds all p -shell nuclei by up to a factor of two), it is also missing e.g. essential spin-orbit couplings. However, starting at NLO the spectra tend to be in qualitative agreement with data. At N^2LO with explicit 3NFs we use SRG evolution to improve convergence of the NCCI calculations. The dependence of the excitation energies on the SRG parameter α is negligible, much smaller than the $\hbar\omega$ dependence, as can be seen in the right-most panels of Fig. 3. Generally, inclusion of the 3NFs improves agreement with experiment (see also Fig. 9 of Ref. [14]). In particular, we see in Fig. 3 that the excitation energy of the 3^{+} state of ^6Li moves slightly closer to experiment; and in ^7Li the $\frac{7}{2}^{-}$ also moves slightly closer to experiment. Furthermore the second $\frac{5}{2}^{-}$ state becomes much better converged while the first $\frac{5}{2}^{-}$ exhibits a persistent $\hbar\omega$ dependence, suggesting that the first $\frac{5}{2}^{-}$ is broad, and the second narrow, both in agreement with data.

In Fig. 4 we show the low-lying positive-parity spectra for ^8Li , ^8Be , and ^{10}Be at N^2LO with explicit 3NFs, SRG evolved to $\alpha = 0.04 \text{ fm}^4$ (solid) and 0.08 fm^4 (dashed). Again, the SRG dependence is negligible compared to the $\hbar\omega$ dependence, except for the high-lying pairs of 2^{+} , 1^{+} , and 3^{+} states in ^8Be ; given this SRG dependence, the spectrum of ^8Be is in quite reasonable agreement with the data. For ^8Li we do find the known narrow 1^{+} , 3^{+} , and 4^{+} states, as well as two poorly converged (i.e. broad) 1^{+} states, all in reasonable agreement with experiment; in addition we find one 0^{+} state, as well as two 2^{+} states, all poorly converged.

The first excited state in ^{10}Be , with $J^P = 2^+$, is quite well converged, and in excellent agreement with the experimental excitation energy. We also do find two additional 2^+ states among the lowest five states in qualitative agreement with data, but not as well converged. However, we do not find any low-lying 0^+ state in our calculations, in contrast to experiment; we will come back to this when discussing ^{12}C below. Furthermore, our calculations suggest that there is a 1^+ state between the second and third 2^+ excited state.

The low-lying spectra for ^{10}B up to N^2LO are shown in Fig. 5; in addition to the ground state 3^+ , two low-lying 1^+ states, and a low-lying 2^+ , there is also the 0^+ analog state of the ground state of ^{10}Be which is not shown. At LO the calculated spectrum does not look like the experimental spectrum at all: the lowest state is a 1^+ state, followed by three nearly degenerate states, with $J^P = 2^+$, 3^+ , and 1^+ , respectively, at excitation energies of about 6 MeV. At NLO and NN-only N^2LO the agreement with experiment is noticeably better, except for the ordering

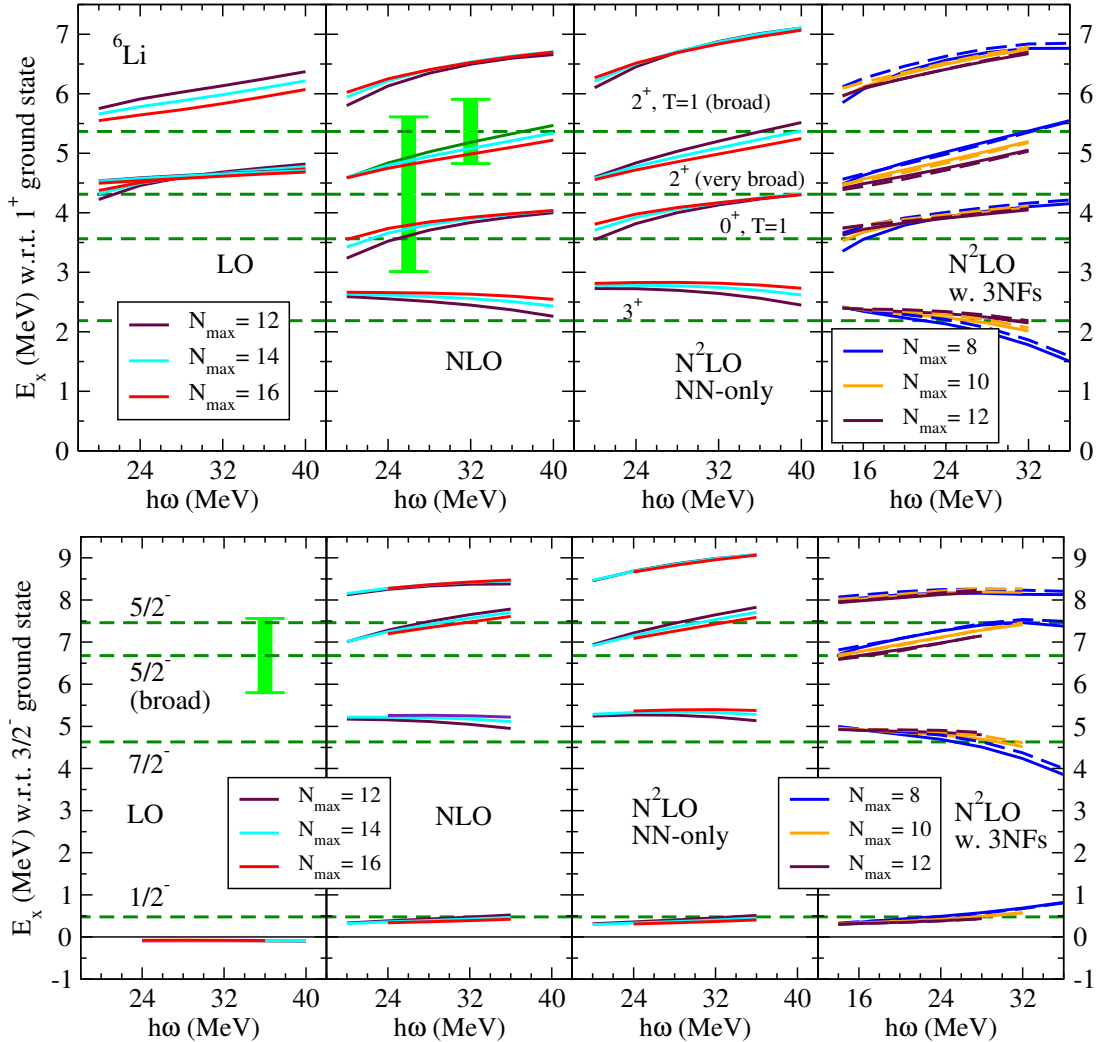


Figure 3. (Color online) Calculated excitation spectrum of ^6Li (top) and ^7Li (bottom) using chiral LO, NLO, and N^2LO interactions at $R = 1.0$ fm as function of the basis HO parameter $\hbar\omega$ for $N_{\text{max}} = 12$ to 16 for NN-only potentials (left 3 panels) and at N^2LO w. 3NFs, SRG-evolved to $\alpha = 0.04$ fm 4 (solid) and $\alpha = 0.08$ fm 4 (dashed) for $N_{\text{max}} = 8$ to 12 (right-most panels). The dashed horizontal lines are the experimental values [28].

of the 3^+ ground state and the lowest 1^+ state. This is a known issue, and the general consensus is that 3NFs are needed to achieve the proper 3^+ ground state for ^{10}B [19, 25]. Indeed, adding the 3NFs at N^2LO does give the correct ground state, followed by two 1^+ states with excitation energies of a few MeV. However, these two low-lying 1^+ states mix, with the amount of mixing strongly dependent on the basis $\hbar\omega$ and N_{max} parameters, which makes it difficult to extract actual excitation energies for these two states [25]. The lowest 2^+ is in reasonable agreement

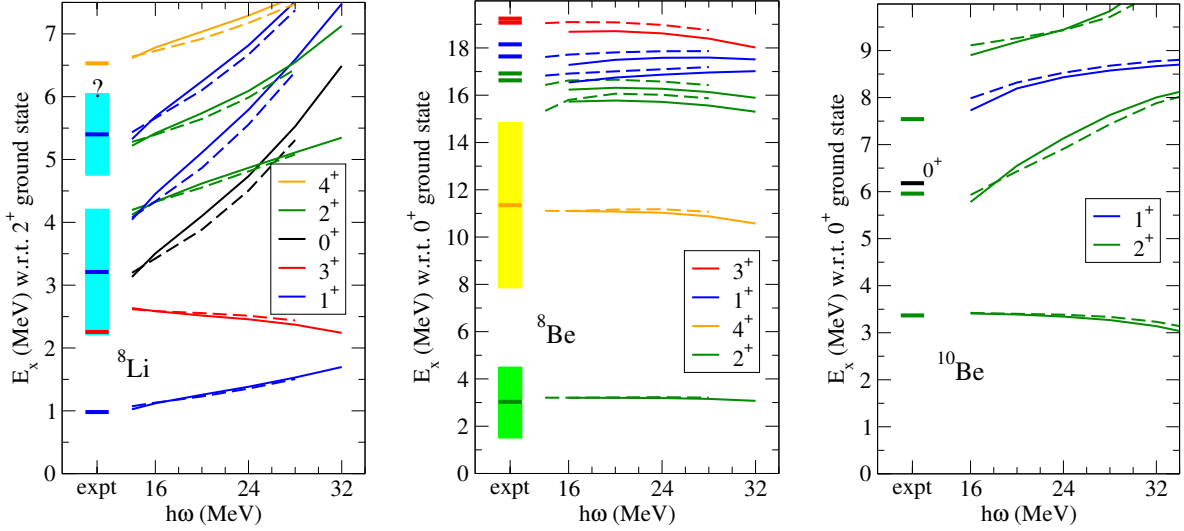


Figure 4. (Color online) Positive-parity excitation spectra of ^8Li , ^8Be , and ^{10}Be using the chiral N^2LO interaction w. 3NFs, SRG-evolved to $\alpha = 0.04 \text{ fm}^4$ (solid) and $\alpha = 0.08 \text{ fm}^4$ (dashed), as function of the basis HO parameter $\hbar\omega$, with $N_{\text{max}} = 10$ for ^8Li and ^8Be and $N_{\text{max}} = 8$ for ^{10}Be . Experimental levels from ENSDF, Ref. [29].

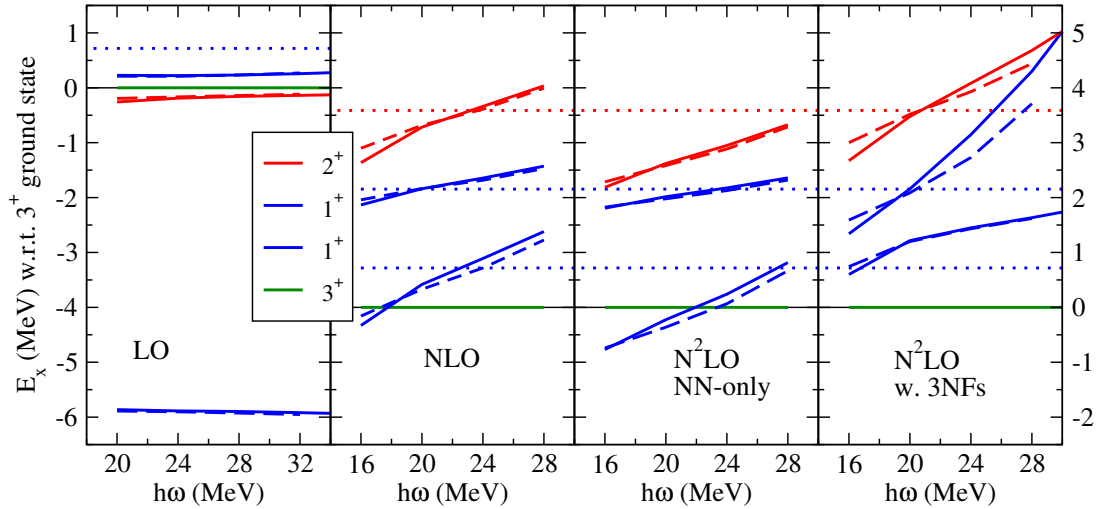


Figure 5. (Color online) Calculated positive-parity excitation spectrum of ^{10}B using chiral LO, NLO, and N^2LO interactions at $R = 1.0 \text{ fm}$ as function of the basis HO parameter at $N_{\text{max}} = 8$ for NN-only potentials (left 3 panels) and for N^2LO w. 3NFs (right-most panel), all SRG-evolved to $\alpha = 0.04 \text{ fm}^4$ (solid) and $\alpha = 0.08 \text{ fm}^4$ (dashed). Note the different vertical offset for the LO panel. The dotted horizontal lines are the experimental values [29].

with the data at N²LO with 3NFs.

Finally, in Fig. 6 we show the low-lying positive-parity spectra for ¹²B and ¹²C. Again, at LO the spectra do not agree with experiment; furthermore, we do not find the Hoyle state in ¹²C (nor any of its rotational excitations) due to the known limitations of the HO basis [31]. Furthermore, our spectra at NLO and N²LO show a significant sensitivity to the chiral order, as well as the 3NFs at N²LO, for both of these two nuclei.

In particular, at N²LO with 3NFs the first excited 2⁺ state in ¹²B becomes the ground state in our calculations, and the splitting between this state and the other excited states is significantly too large. On the other hand, the energy differences of the 0⁺, the second 2⁺, the 1⁺, and the 3⁺ relative to the lowest 1⁺ state are in better agreement with 3NFs than without 3NFs at N²LO. Possibly even more puzzling, though not surprising, is the lowest 1⁺ excited state in ¹²C [32]. At NLO it is in reasonable agreement with experiment, just below the 4⁺ rotational excitation

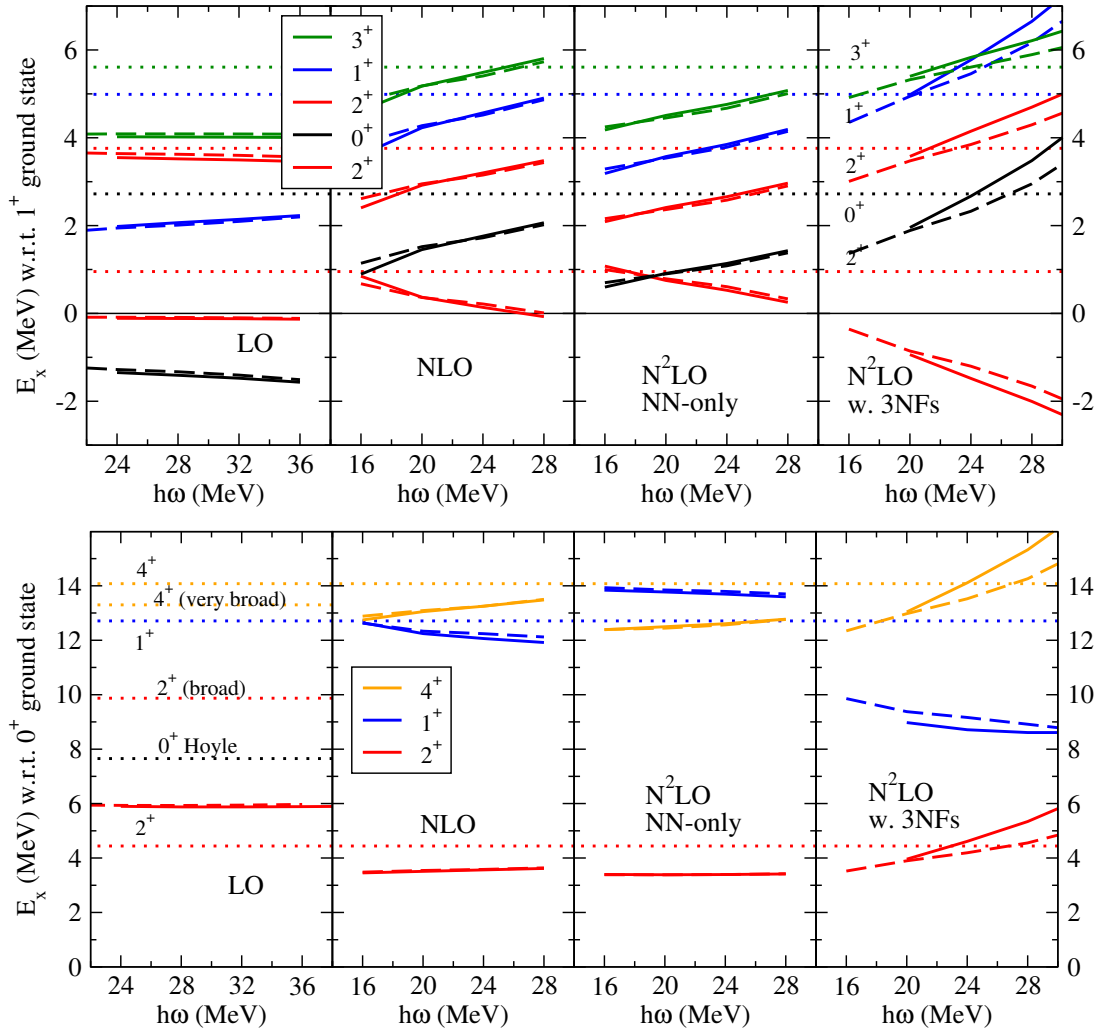


Figure 6. (Color online) Calculated positive-parity excitation spectrum of ¹²B (top) and ¹²C (bottom) using chiral LO, NLO, and N²LO interactions at $R = 1.0$ fm as function of the basis HO parameter at $N_{\text{max}} = 8$ for NN-only potentials (left 3 panels) and for N²LO w. 3NFs (right-most panel), all SRG-evolved to $\alpha = 0.04$ fm⁴ (solid) and $\alpha = 0.08$ fm⁴ (dashed). The dotted horizontal lines are the experimental values [30].

of the ground state; at N²LO without 3NFs, the order of the 1⁺ and the 4⁺ is reversed; and including the 3NFs at N²LO reduces the excitation energy of the 1⁺ by about 5 MeV, destroying the qualitative agreement with experiment. Note that this shift due to the 3NFs is significantly larger than that for the 2⁺ state in ¹²B, which is of the order of 2 MeV.

In conclusion most spectra for *p*-shell nuclei up to $A = 12$, calculated at N²LO with 3NFs, agree reasonably well with the experimental data, in particular for narrow states. The exceptions are two states, in ¹²B and ¹²C respectively. The low-lying spectra of ¹⁰B and ¹²B, together with the excitation energy of the lowest 1⁺ state in ¹²C, could play a critical role in determining accurate NN and 3N interactions for the upper *p*-shell and beyond. Indeed, both the 2⁺ state in ¹²B and the 1⁺ state in ¹²C are sensitive to e.g. the LECs c_D and c_E .

Acknowledgments

This work was supported by the US Department of Energy under Grant No. DE-SC0018223 (SciDAC-4/NUCLEI) and the Fundação de Amparo à Pesquisa do Estado de São Paulo, Brazil (FAPESP) under Grant No. 2017/19371-0. This research used resources of the National Energy Research Scientific Computing Center (NERSC) and the Argonne Leadership Computing Facility (ALCF), which are US Department of Energy Office of Science user facilities, supported under Contracts No. DE-AC02-05CH11231 and No. DE-AC02-06CH11357, and computing resources provided under the INCITE award ‘Nuclear Structure and Nuclear Reactions’ from the US Department of Energy, Office of Advanced Scientific Computing Research.

References

- [1] Barrett B R, Navrátil P and Vary J P 2013 *Prog. Part. Nucl. Phys.* **69** 131
- [2] Maris P, Vary J P and Shirokov A M 2009 *Phys. Rev.* **C79** 014308
- [3] Coon S A, Avetian M I, Kruse M K G, van Kolck U, Maris P and Vary J P 2012 *Phys. Rev.* **C86** 054002
- [4] Furnstahl R J, Hagen G and Papenbrock T 2012 *Phys. Rev.* **C86** 031301
- [5] More S N, Ekström A, Furnstahl R J, Hagen G and Papenbrock T 2013 *Phys. Rev.* **C87** 044326
- [6] Wendt K A, Forssén C, Papenbrock T and Sääf D 2015 *Phys. Rev.* **C91** 061301
- [7] Aktulga H M, Yang C, Ng E G, Maris P and Vary J P 2014 *Concurrency Computat.: Pract. Exper.* **26** 2631
- [8] Shao M, Aktulga H, Yang C, Ng E G, Maris P and Vary J P 2018 *Comput. Phys. Commun.* **222** 1
- [9] Weinberg S 1990 *Phys. Lett.* **B251** 288
- [10] Epelbaum E, Hammer H W and Meißner U G 2009 *Rev. Mod. Phys.* **81** 1773
- [11] Machleidt R and Entem D R 2011 *Phys. Rept.* **503** 1
- [12] Binder S *et al.* (LENPIC) 2016 *Phys. Rev.* **C93** 044002
- [13] Binder S *et al.* (LENPIC) 2018 *Phys. Rev.* **C98** 014002
- [14] Epelbaum E *et al.* (LENPIC) 2019 *Phys. Rev.* **C99** 024313
- [15] Epelbaum E, Krebs H and Meißner U G 2015 *Eur. Phys. J.* **A51** 53
- [16] Epelbaum E, Krebs H and Meißner U G 2015 *Phys. Rev. Lett.* **115** 122301
- [17] Epelbaum E, Nogga A, Gloeckle W, Kamada H, Meißner U G and Witała H 2002 *Phys. Rev.* **C66** 064001
- [18] Nogga A, Navrátil P, Barrett B and Vary J P 2006 *Phys. Rev.* **C73** 064002
- [19] Navrátil P, Gueorguiev V G, Vary J P, Ormand W E and Nogga A 2007 *Phys. Rev. Lett.* **99** 042501
- [20] Gazit D, Quaglioni S and Navrátil P 2009 *Phys. Rev. Lett.* **103** 102502
- [21] Bogner S K, Furnstahl R J, Maris P, Perry R J, Schwenk A and Vary J P 2008 *Nucl. Phys.* **A801** 21
- [22] Bogner S K, Furnstahl R J and Schwenk A 2010 *Prog. Part. Nucl. Phys.* **65** 94
- [23] Roth R, Calci A, Langhammer J and Binder S 2014 *Phys. Rev.* **C90** 024325
- [24] Maris P and Vary J P 2013 *Int. J. Mod. Phys.* **E22** 1330016
- [25] Jurgenson E D, Maris P, Furnstahl R J, Navrátil P, Ormand W E and Vary J P 2013 *Phys. Rev.* **C87** 054312
- [26] Audi G, Wapstra A and Thibault C 2003 *Nucl. Phys.* **A729** 337
- [27] Calci A, Navrátil P, Roth R, Dohet-Eraly J, Quaglioni S and Hupin G 2016 *Phys. Rev. Lett.* **117** 242501
- [28] Tilley D *et al.* 2002 *Nucl. Phys.* **A708** 3
- [29] Tilley D, Kelley J, Godwin J, Millener D, Purcell J, Sheu C and Weller H 2004 *Nucl. Phys.* **A745** 155
- [30] Kelley J, Purcell J and Sheu C 2017 *Nucl. Phys.* **A968** 71
- [31] Chernykh M, Feldmeier H, Neff T, von Neumann-Cosel P and Richter A 2007 *Phys. Rev. Lett.* **98** 032501
- [32] Maris P, Vary J P, Calci A, Langhammer J, Binder S and Roth R 2014 *Phys. Rev.* **C90** 014314